

Non-local Correlation Effects in Fermionic Many-Body Systems: Overcoming the Non-causality Problem

Steffen Backes^{1,2,3,*}, Jae-Hoon Sim¹, and Silke Biermann^{1,2,3,4}

¹*CPHT, CNRS, Ecole Polytechnique, Institut Polytechnique de Paris, Route de Saclay, 91128 Palaiseau, France*

²*Collège de France, 11 place Marcelin Berthelot, 75005 Paris, France*

³*European Theoretical Spectroscopy Facility, 91128 Palaiseau, France, Europe and*

⁴*Department of Physics, Division of Mathematical Physics, Lund University, Professorsgatan 1, 22363 Lund, Sweden*

(Dated: February 18, 2022)

Motivated by the intriguing physics of quasi-2d fermionic systems, such as high-temperature superconducting oxides, layered transition metal chalcogenides or surface or interface systems, the development of many-body computational methods geared at including both local and non-local electronic correlations has become a rapidly evolving field. It has been realized, however, that the success of such methods can be hampered by the emergence of noncausal features in the effective or observable quantities involved. Here, we present a new approach of extending local many-body techniques such as dynamical mean field theory (DMFT) to nonlocal correlations, which preserves causality and has a physically intuitive interpretation. Our strategy has implications for the general class of DMFT-inspired many-body methods, and can be adapted to cluster, dual boson or dual fermion techniques with minimal effort.

Electronic correlations arising from the Coulomb repulsion between electrons in a solid are at the heart of the astounding variety of emergent phenomena in condensed matter, ranging from exotic transport phenomena such as superconductivity to unconventional ordering phenomena involving spin, charge or orbital degrees of freedom. Even in simplified lattice models with purely local interactions, the Coulomb term requires refined approximations, such as dynamical mean-field theory (DMFT)[1–3]. This method proved to be highly successful in describing various effects of electronic correlations like the metal-insulator transition in transition metal compounds, Kondo physics, magnetic properties or superconductivity[2, 4–15].

Still, as a local approximation DMFT is inadequate for systems where nonlocal correlations and interactions are important. Thus, various methods aiming to reintroduce an approximate momentum dependence of the self-energy have been developed. Cluster extensions[2, 4, 7] or the dynamical cluster approximation (DCA)[16] introduce short range correlations, the dynamical vertex approximation (DGA)[17–19], TRILEX[20] or QUADRILEX[21] schemes incorporate local but dynamical irreducible vertices, while dual fermion[22] or boson[23] approaches perform a diagrammatic expansion around the DMFT solution to reintroduce momentum dependent correlation effects. Extended DMFT (EDMFT)[24] incorporates screening effects of nonlocal interactions, while the combined GW+EDMFT method[25–33] includes nonlocal screening and correlations on the level of the random phase and GW approximation. In this general approach one approximates the full self-energy by a sum of the local contribution $\Sigma_{loc}(\omega)$ generated from an effective impurity model, and a non-local part $\Sigma_{nonloc}(k, \omega)$, which for example can be ob-

tained from a perturbative approach like the *GW* approximation (GW+DMFT)[25, 31, 34], the fluctuation-exchange approximation (FLEX+DMFT)[15, 35], second order diagrams ($\Sigma^{(2)}$ +DMFT)[36, 37] or exact diagonalization (ED+DMFT)[38]. A systematic formulation for such combination of local and nonlocal self-energies is provided by the self-energy embedding theory (SEET)[36, 39]. While these methods proved highly successful in describing nonlocal phenomena like pseudogap physics, magnetism, superconductivity and charge order[40–47], it has recently been realized that the combination of local techniques with nonlocal corrections can lead to noncausal, i.e. unphysical results, hampering the predictive power and applicability of the methods.

In this Letter we present a new self-consistent scheme for including nonlocal correlation effects into local theories, which preserves causality and has a transparent physical interpretation. In the limit of a local self-energy the standard DMFT equations are recovered. While we focus on GW+DMFT-like methods, this approach readily applies to cluster methods, and in general to all methods that include a feedback of the nonlocal on the local self-energy, like self-consistent dual boson, fermion or DGA[19] techniques. We benchmark our technique on an exactly solvable model, a two-site Hubbard dimer.

Noncausal behavior of physical quantities such as the Green's function, self-energy, hybridization or effective Weiss mean field corresponds to negative spectral weight in the spectral representation of their diagonal elements. In extensions of the dynamical cluster approximation(DCA) where the self-energy is interpolated to a continuous momentum-dependence, violation of causality has been reported[48]. A failure of causality in GW+DMFT was reported for the screened Coulomb interaction in [49] and in a two-atom system in

the strongly correlated regime [50]. Here, the effective hybridization of the impurity model became significantly noncausal. For real materials Refs.[51–53] reported a general noncausal effective hybridization and interaction in GW+EDMFT. While non-causality was not detected in observable quantities [52], inclusion of nonlocal correlations and screening appeared to lead to a decrease of local correlations in transition metal oxides compared to a local approximation. A spurious reduction of correlation strength due to a feedback of nonlocal correlations was also reported in self-consistent dual-fermion[54, 55] and DGA[19] calculations, albeit causality violation was not investigated.

The problem of noncausality in these approaches is general and not related to the approximations involved. Indeed, it arises from imposing that the local part of the Green's function can be generated from a local model. This can be seen from the exact solution of a two-site Hubbard dimer with intersite hopping t and onsite interaction U . Using $G_{imp} = G_{loc}$ the effective single-site impurity hybridization can be evaluated analytically as

$$\Delta(\omega) = \frac{(t - \Sigma_{inter}(\omega))^2}{\omega + \mu - \Sigma_{loc}(\omega)}, \quad (1)$$

where Σ_{inter} is the intersite and Σ_{loc} the onsite self-energy. While this constitutes a causal hybridization in the DMFT limit $\Sigma_{inter} = 0$, noncausal spectral weight $-\text{Im}[\Delta] < 0$ emerges in the general case including the exact solution, due to the imaginary term Σ_{inter} in the nominator (see Fig.1 below). Thus, the noncausality problem due to the inclusion of a nonlocal self-energy is inherent to the commonly used form of the self-consistency equations, as even the exact solution generates a noncausal impurity model.

For simplicity we consider a single-orbital fermionic Hubbard model with intersite hoppings t_{ij} , chemical potential μ , and on-site interaction U . (The generalization to the multi-orbital case is straight forward.) The full action S for this system is given by

$$S = \int_0^\beta d\tau \sum_{i\sigma} c_{i\sigma}^*(\tau) \left[\frac{\partial}{\partial \tau} - \mu \right] c_{i\sigma}(\tau) - \sum_{ij,\sigma} \int_0^\beta d\tau t_{ij} c_{i\sigma}^*(\tau) c_{j\sigma}(\tau) + \sum_i U \int_0^\beta d\tau n_{i\uparrow}(\tau) n_{i\downarrow}(\tau), \quad (2)$$

where $c_{i\sigma}(\tau), c_{i\sigma}^*(\tau)$ are anticommuting Grassman variables, $n_{i\sigma}(\tau) = c_{i\sigma}^*(\tau) c_{i\sigma}(\tau)$ and $n_i(\tau) = n_{i\uparrow}(\tau) + n_{i\downarrow}(\tau)$. Following the idea of the cavity construction as outlined in Ref.2, we split the action S into three contributions $S = S_0 + \Delta S + S^{(0)}$, where S_0 is the term that contains

only the local quantities on site $i = 0$, ΔS contains all contributions that couple the site $i = 0$ to all other sites, and $S^{(0)}$ contains all the contributions of the lattice with site $i = 0$ and its bonds connecting it being removed. Integrating out all the degrees of freedom except the ones on site $i = 0$ one obtains an effective action of the form

$$S_{eff} = S_0 - \sum_{n=1}^{\infty} \frac{(-1)^n}{n!} \langle (\Delta S)^n \rangle^{(0)}, \quad (3)$$

where $\langle \rangle^{(0)}$ indicates a trace over the system without the site $i = 0$. In Refs.2, 56, and 57 it has been shown that for infinite lattice connectivity and a dimensional rescaling of the hopping parameters only the term $n = 2$ survives in the effective action. Therefore, in this limit the effective action reduces to the local part and the second order contribution, which takes the form of an effective impurity action parameterized by the effective Weiss field

$$\mathcal{G}^{-1}(\tau_1 - \tau_2) = -\delta(\tau_1 - \tau_2) \left[\frac{\partial}{\partial \tau} - \mu + t_{00} \right] - \sum_{ij \neq 0} t_{0i} t_{j0} G_{ij}^{(0)}(\tau_1 - \tau_2). \quad (4)$$

Inserting the equality $G_{ij}^{(0)} = G_{ij} - G_{i0} G_{00}^{-1} G_{0j}$ into Eq.(4) and performing a Fourier transform, we obtain

$$\mathcal{G}^{-1} = i\omega + \mu - \langle \epsilon \rangle - \Delta(i\omega) \quad \text{with } \Delta(i\omega) = \langle \epsilon G \epsilon \rangle - \langle \epsilon G \rangle \langle G \rangle^{-1} \langle G \epsilon \rangle, \quad (5)$$

where the spin index σ is suppressed for readability. The bracket $\langle \rangle = \int dk$ indicates a local projection of the corresponding lattice quantity. $\epsilon(k)$ is the Fourier transform of the hoppings t_{ij} . We point out that Eq.(4) and Eq.(5) are equivalent, even when the self-energy is nonlocal, and the only approximation has been performed on the effective action in Eq.(3). Most importantly, since $G_{ij}^{(0)}$ is a causal Green's function by definition, the resulting Weiss field \mathcal{G} and hybridization in this form are also causal. While in infinite dimensions the self-energy indeed does become local, for finite dimensions this constitutes an additional approximation, which simplifies Eq.(5) to the local Dyson equation $\mathcal{G}^{-1} = \langle G \rangle^{-1} + \langle \Sigma \rangle$ used in DMFT and its nonlocal extensions.

Now we explicitly consider a momentum dependent self-energy $\Sigma(k, i\omega)$ in the interacting Green's function

$$G(k, i\omega) = [i\omega + \mu - \epsilon(k) - \Sigma(k, i\omega)]^{-1}. \quad (6)$$

Rewriting Eq.(5) without a local self-energy approximation we arrive at a generalized cavity equation

$$\mathcal{G}^{-1} = \langle G \rangle^{-1} + \langle \Sigma \rangle - \left(\langle \Sigma G \Sigma \rangle - \langle \Sigma G \rangle \langle G \rangle^{-1} \langle G \Sigma \rangle + 2 \langle \Sigma \rangle - \langle \Sigma G \rangle \langle G \rangle^{-1} - \langle G \rangle^{-1} \langle G \Sigma \rangle \right). \quad (7)$$

Here one identifies the first two terms as the local Dyson equation, but with an additional correction term. As an exact rewriting of the causal equation (5), this expression is causal as well. Since the Dyson equation yields a noncausal bath in general as demonstrated in Eq(1), the correction term is responsible for ensuring causality in the case of a nonlocal self-energy. This result can be extended to nonlocal screening and interactions, resulting in very similar equations for the effective impurity interaction [58, 59]. Neglecting the momentum-dependence of the self-energy in the DMFT limit the local projection factorizes $\langle G\Sigma \rangle = \langle G \rangle \langle \Sigma \rangle$ and the correction terms vanishes, recovering the DMFT local Dyson equation. Even when the nonlocal self-energy is frequency-independent, this correction term does not vanish, e.g. in the case of a static Fock-like self-energy, but still modifies the bath.

GW+DMFT and related self-consistent schemes that include a nonlocal self-energy and enforce $G_{loc} = G_{imp}$, i.e. the impurity bath $\mathcal{G}(i\omega)$ is given by the local Dyson equation, will in general produce a noncausal solution, unless the correction term above is included. In cluster approaches such as cluster-DMFT, where the self-energy is local on a cluster and correlations within the cluster are included as offdiagonal elements, the local Dyson equation is causal. If the self-energy is periodized during the self-consistency to reestablish translational invariance, it picks up a true momentum dependence and noncausality emerges, unless the correction term is included. Similarly, the noncausality problem in the DCA for momentum-interpolated self-energies can be remedied by inclusion of the additional term above.

The correction term has a clear physical interpretation: redefining the hopping amplitudes such that they absorb the nonlocal self-energy $\hat{t}_{ij} = t_{ij} + \Sigma_{ij}$, $i \neq j$, one recovers the local Dyson equation, since the remaining self-energy is purely local. This implies that the Dyson equation dresses all intersite hoppings with the nonlocal self-energy, including the ones connecting the impurity with the bath t_{i0}, t_{0j} . But the cavity construction and Eq.(4) require the bare hopping amplitudes for connecting the impurity with the bath. Therefore, the additional correction term in Eq.(7) removes the nonlocal self-energy contribution dressing the bath-impurity hoppings, which would otherwise result in a 'double-counting' of the nonlocal self-energy effects on the local correlations.

When deriving DMFT within a functional approach[6, 60], the resulting stationarity condition $G_{loc} = G_{imp}$ is equivalent to the cavity construction in infinite dimensions, and thus the bath is always related to a physical lattice via a second order approximation of the effective action. When including a nonlocal self-energy as in the standard GW+DMFT scheme[31, 52] or related methods, this connection to a lattice via the cavity construction is sacrificed. Here, via Eq.(7) we restrict ourselves to the solutions that retain the relation to a physical lattice via the cavity construction, and thus preserve

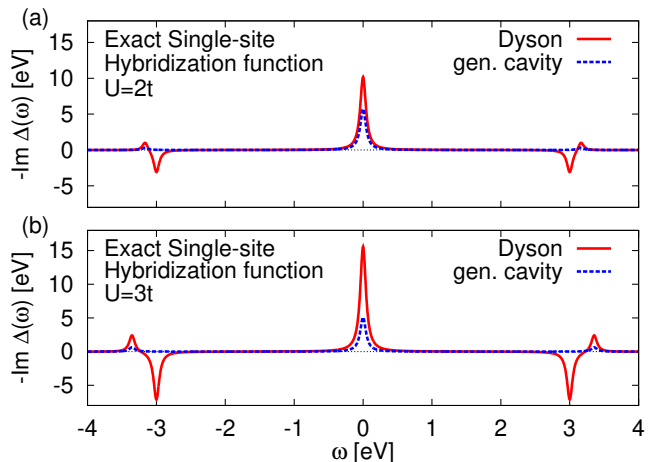


FIG. 1. The effective single-site impurity hybridization for the exact solution of a two-site dimer at half filling for the interaction (a) $U = 2t$ and (b) $U = 3t$. Noncausal spectral weight is evident by negative values of $-\text{Im}\Delta$ in the bath generated from Eq.(1). The generalized cavity equation Eq.(8) generates a bath that is always causal. The hybridization at $\omega = 0$ is overestimated in the Dyson equation, leading to a reduced strength of electronic correlations.

causality. This approach results in $G_{imp} \neq G_{loc}$, as can be seen by comparing Eq.(7) with the impurity Dyson equation, a feature common to diagrammatic extensions of DMFT[61–64]. Now the impurity Green's function becomes an auxiliary, albeit always causal quantity that generates an approximation to the local self-energy. Assuming $\Sigma_{loc} = \Sigma_{imp}$, this establishes the self-consistency relation for the local self-energy used to solve Eq.(7) iteratively. For a given Σ_{nonloc} the resulting scheme has the following form:

- 1) Make a starting guess for Σ_{loc} .
- 2) Deduce $G(k, i\omega)$ from Eq.(6) with $\Sigma = \Sigma_{loc} + \Sigma_{nonloc}$
- 3) Obtain $\Delta(i\omega)$ and $\mathcal{G}(i\omega)$ from Eq.(5)
- 4) Solve impurity model to obtain G_{imp} and deduce $\Sigma_{imp} = \mathcal{G}^{-1} - G_{imp}^{-1}$
- 5) Iterate using $\Sigma_{loc} = \Sigma_{imp}$ until self-consistency.

We now apply this scheme to the two-site dimer. Using Eq.(5) or Eq.(7) we analytically evaluate the effective single-site hybridization and obtain

$$\Delta(\omega) = \frac{t^2}{\omega + \mu - \Sigma_{loc}(\omega)}. \quad (8)$$

This expression is always causal and the intersite hopping is not renormalized by the intersite self-energy, in contrast to the Dyson equation in Eq.(1). This confirms our interpretation of the correction term in Eq.(7), which ensures that the impurity is coupled to the bath via the bare hopping t . As there is only one bond in the dimer, the bath consists only of the other site, thus no intersite self-energy enters the bath. The Dyson equation includes the intersite self-energy on the bond, which gives rise to

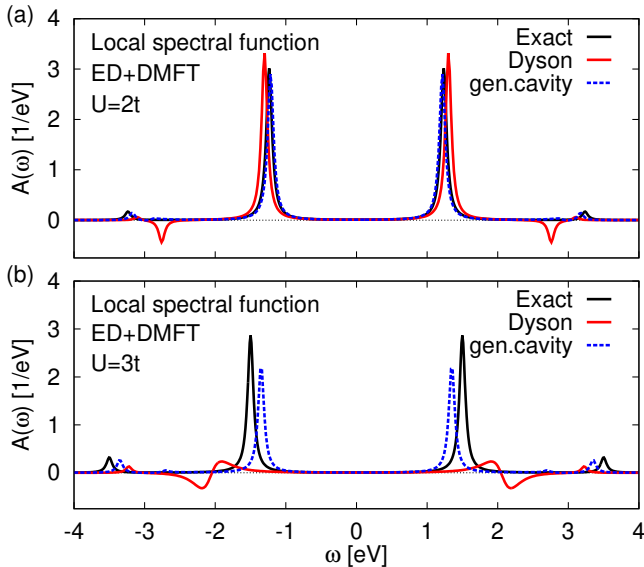


FIG. 2. The ED+DMFT local spectral function for a two-site dimer at half filling, compared to the exact solution for (a) $U = 2t$ and (b) $U = 3t$. The exact form of the nonlocal self-energy has been used. The generalized cavity equations in Eq.(5) reproduce the exact solution well. For small interaction values the Dyson equation generates noncausal spectral weight, and fails completely for $U \gtrsim 3t$, as the Green's function becomes nonanalytic (see explanation in main text).

the noncausal spectral weight, as its effect is similar to a dissipative term in the one-particle Hamiltonian.

In Fig.1 we show the effective single-site impurity hybridization, generated from Eqs.(1) and (8) for $U = 2t$ and $3t$, using the exact self-energy. The Dyson equation generates noncausal spectral weight at $\omega = \pm 3$ eV, enhanced for larger interactions. The new scheme always produces a causal result. At the Fermi level $\omega = 0$ the Dyson equation significantly overestimates the hybridization compared to Eq.(8), which we also observed for other model systems and thus expect to be a general effect. This can explain the reported reduced strength of electronic correlations [19, 48, 52, 54, 55].

In Fig.2 we show converged results for an ED+DMFT scheme, using the exact nonlocal self-energy and determining the local self-energy self-consistently. We employed an exact diagonalization impurity solver allowing for a non-hermitian bath to describe the noncausal impurity hybridization. Both the generalized cavity scheme and Dyson equation agree well with the exact result for $U = 2t$, with the latter showing a slightly worse agreement and noncausal spectral weight. For $U \gtrsim 3t$ the Dyson equation fails completely while the cavity scheme is still in qualitative agreement with the exact solution. The failure of the Dyson equation can be traced back to the poles of the Green's function separating from the real axis and entering the complex plane, corresponding to imaginary Eigenvalues that arise from a noncausal

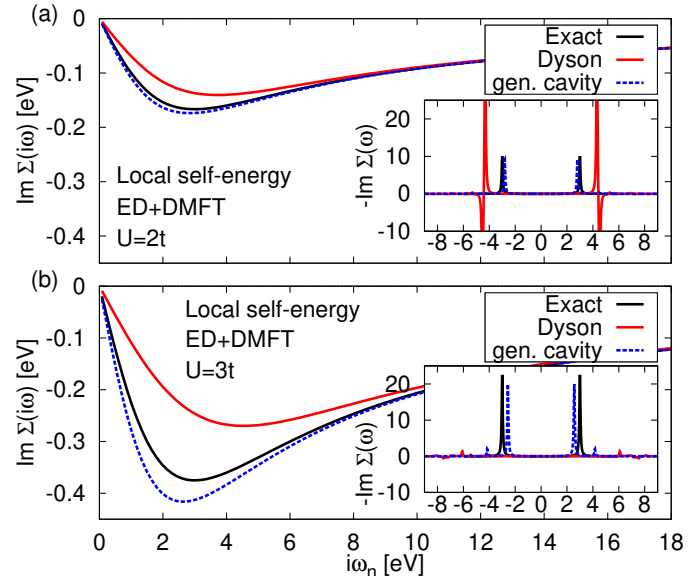


FIG. 3. The local self-energy Σ_{loc} on Matsubara $i\omega_n$ or real frequencies ω (inset) for the dimer as in Fig.2. The generalized cavity equations obtain a self-energy in good agreement with the exact result. The local Dyson equation underestimates the correlation strength, creates a noncausal self-energy and breaks down for $U \gtrsim 3t$ (see explanation in main text).

bath, i.e. nonhermitian hybridization amplitudes[58]. In this case the Green's function is no longer analytic in either the upper/lower complex plane, violating a necessary condition for the Hilbert transform, which connects the spectra on the real to the imaginary Matsubara axis. As a result, analytic continuation such as the maximum entropy method[65] can no longer be applied[58].

This is evident in the local self-energy as well (Fig.(3)). While for the Dyson equation Σ_{loc} vanishes on the real axis for $U \gtrsim 3t$ as all poles have left the real axis, the Matsubara self-energy is finite and shows no obvious abnormal features apart from an underestimation of correlation strength. The lack of any signatures in the Matsubara data makes this especially critical for real materials calculations, where real-frequency impurity solvers are often not feasible, making it impossible to detect such a breakdown of the formalism. The generalized cavity equations instead generate a causal self-energy that agrees well with the exact solution.

We have presented a generalized form of a cavity construction for correlated fermionic systems that explicitly includes both local and nonlocal correlations. The result is an effective impurity problem that has a physically meaningful interpretation and solves the noncausality problem that so far has hampered the development of many-body methods for describing non-local correlations. The method can be readily adapted to any method which incorporates nonlocal self-energies in the form of an effective impurity problem, such as clus-

ter methods, self-consistent dual fermion/boson or DfA techniques. Using a two-site dimer as a benchmark system, the scheme results in causal solutions in very good agreement with the exact result. This provides important progress as compared to current state-of-the-art approaches, which generate noncausal spectral weight, underestimate the correlation strength and violate analyticity. Our scheme can be readily extended to nonlocal screening and interactions, as discussed in the supplementary material [58, 59].

The authors gratefully acknowledge discussions with Hartmut Hafermann, Hong Jiang, Aaram Kim, Benjamin Lenz, and Lucia Reining. This work has been supported by a Consolidator Grant of the European Research Council (Project CorrelMat-617196) and IDRIS/GENCI under project number t2020091393. We are grateful to the CPHT computer support team.

* steffen.backes@polytechnique.edu

- [1] A. Georges and G. Kotliar, Phys. Rev. B **45**, 6479 (1992).
- [2] A. Georges, G. Kotliar, W. Krauth, and M. J. Rozenberg, Rev. Mod. Phys. **68**, 13 (1996).
- [3] D. Vollhardt, AIP Conference Proceedings **1297**, 339 (2010).
- [4] A. I. Lichtenstein and M. I. Katsnelson, Phys. Rev. B **62**, R9283 (2000).
- [5] M. B. Zöfl, I. A. Nekrasov, T. Pruschke, V. I. Anisimov, and J. Keller, Phys. Rev. Lett. **87**, 276403 (2001).
- [6] G. Kotliar, S. Y. Savrasov, K. Haule, V. S. Oudovenko, O. Parcollet, and C. A. Marianetti, Rev. Mod. Phys. **78**, 865 (2006).
- [7] H. Park, K. Haule, and G. Kotliar, Phys. Rev. Lett. **101**, 186403 (2008).
- [8] M. Aichhorn, L. Pourovskii, V. Vildosola, M. Ferrero, O. Parcollet, T. Miyake, A. Georges, and S. Biermann, Phys. Rev. B **80**, 085101 (2009).
- [9] J. Bauer, A. C. Hewson, and N. Dupuis, Phys. Rev. B **79**, 214518 (2009).
- [10] L. de' Medici, S. R. Hassan, M. Capone, and X. Dai, Phys. Rev. Lett. **102**, 126401 (2009).
- [11] K. Haule and G. Kotliar, New Journal of Physics **11**, 025021 (2009).
- [12] P. Hansmann, R. Arita, A. Toschi, S. Sakai, G. Sangiovanni, and K. Held, Phys. Rev. Lett. **104**, 197002 (2010).
- [13] Z. P. Yin, K. Haule, and G. Kotliar, Nature Materials **10**, 932 (2011).
- [14] S. Biermann, Dynamical mean field theory-based electronic structure calculations for correlated materials, in *First Principles Approaches to Spectroscopic Properties of Complex Materials*, edited by C. Di Valentin, S. Botti, and M. Cococcioni (Springer Berlin Heidelberg, Berlin, Heidelberg, 2014) pp. 303–345.
- [15] M. Kitatani, N. Tsuji, and H. Aoki, Phys. Rev. B **92**, 085104 (2015).
- [16] M. H. Hettler, A. N. Tahvildar-Zadeh, M. Jarrell, T. Pruschke, and H. R. Krishnamurthy, Phys. Rev. B **58**, R7475 (1998).
- [17] A. Toschi, A. A. Katanin, and K. Held, Phys. Rev. B **75**, 045118 (2007).
- [18] A. Galler, P. Thunström, P. Gunacker, J. M. Tomczak, and K. Held, Phys. Rev. B **95**, 115107 (2017).
- [19] J. Kaufmann, C. Eckhardt, M. Pickem, M. Kitatani, A. Kauch, and K. Held, Self-consistent ab initio d γ a approach (2020), arXiv:2010.03938 [cond-mat.str-el].
- [20] T. Ayrál and O. Parcollet, Phys. Rev. B **92**, 115109 (2015).
- [21] T. Ayrál and O. Parcollet, Phys. Rev. B **94**, 075159 (2016).
- [22] A. N. Rubtsov, M. I. Katsnelson, and A. I. Lichtenstein, Phys. Rev. B **77**, 033101 (2008).
- [23] A. Rubtsov, M. Katsnelson, and A. Lichtenstein, Annals of Physics **327**, 1320 (2012).
- [24] P. Sun and G. Kotliar, Phys. Rev. B **66**, 085120 (2002).
- [25] S. Biermann, F. Aryasetiawan, and A. Georges, Phys. Rev. Lett. **90**, 086402 (2003).
- [26] J. M. Tomczak, M. Casula, T. Miyake, F. Aryasetiawan, and S. Biermann, EPL (Europhysics Letters) **100**, 67001 (2012).
- [27] T. Ayrál, P. Werner, and S. Biermann, Phys. Rev. Lett. **109**, 226401 (2012).
- [28] T. Ayrál, S. Biermann, and P. Werner, Phys. Rev. B **87**, 125149 (2013).
- [29] P. Hansmann, T. Ayrál, L. Vaugier, P. Werner, and S. Biermann, Phys. Rev. Lett. **110**, 166401 (2013).
- [30] L. Huang, T. Ayrál, S. Biermann, and P. Werner, Phys. Rev. B **90**, 195114 (2014).
- [31] S. Biermann, Journal of Physics: Condensed Matter **26**, 173202 (2014).
- [32] J. M. Tomczak, M. Casula, T. Miyake, and S. Biermann, Phys. Rev. B **90**, 165138 (2014).
- [33] T. Ayrál, S. Biermann, P. Werner, and L. Boehnke, Phys. Rev. B **95**, 245130 (2017).
- [34] F. Nilsson, L. Boehnke, P. Werner, and F. Aryasetiawan, Phys. Rev. Materials **1**, 043803 (2017).
- [35] M. Kitatani, N. Tsuji, and H. Aoki, Phys. Rev. B **92**, 085104 (2015).
- [36] A. A. Kananenka, E. Gull, and D. Zgid, Phys. Rev. B **91**, 121111(R) (2015).
- [37] J. Gukelberger, L. Huang, and P. Werner, Phys. Rev. B **91**, 235114 (2015).
- [38] A. Liebsch and H. Ishida, Journal of Physics: Condensed Matter **24**, 053201 (2011).
- [39] D. Zgid and E. Gull, New Journal of Physics **19**, 023047 (2017).
- [40] Y. Z. Zhang and M. Imada, Phys. Rev. B **76**, 045108 (2007).
- [41] P. Staar, T. Maier, and T. C. Schulthess, Phys. Rev. B **88**, 115101 (2013).
- [42] T. Ayrál and O. Parcollet, Phys. Rev. B **93**, 235124 (2016).
- [43] E. A. Stepanov, A. Huber, E. G. C. P. van Loon, A. I. Lichtenstein, and M. I. Katsnelson, Phys. Rev. B **94**, 205110 (2016).
- [44] L. Sponza, P. Pisanti, A. Vishina, D. Pashov, C. Weber, M. van Schilfgaarde, S. Acharya, J. Vidal, and G. Kotliar, Phys. Rev. B **95**, 041112(R) (2017).
- [45] J. Vučićević, T. Ayrál, and O. Parcollet, Phys. Rev. B **96**, 104504 (2017).
- [46] B. Lenz, C. Martins, and S. Biermann, Journal of Physics: Condensed Matter **31**, 293001 (2019).
- [47] S. Li and E. Gull, Phys. Rev. Research **2**, 013295 (2020).
- [48] U. R. Hähner, T. A. Maier, and T. C. Schulthess, Phys.

- Rev. B **101**, 195114 (2020).
- [49] S. Chauvin, T. Ayrat, L. Reining, and S. Biermann, Non-local coulomb interactions on the triangular lattice in the high-doping regime: Spectra and charge dynamics from extended dynamical mean field theory (2017), arXiv:1709.07901 [cond-mat.str-el].
- [50] J. Lee and K. Haule, Phys. Rev. B **95**, 155104 (2017).
- [51] L. Boehnke, F. Nilsson, F. Aryasetiawan, and P. Werner, Phys. Rev. B **94**, 201106(R) (2016).
- [52] F. Nilsson, L. Boehnke, P. Werner, and F. Aryasetiawan, Phys. Rev. Materials **1**, 043803 (2017).
- [53] F. Petocchi, F. Nilsson, F. Aryasetiawan, and P. Werner, Phys. Rev. Research **2**, 013191 (2020).
- [54] T. Ribic, P. Gunacker, and K. Held, Phys. Rev. B **98**, 125106 (2018).
- [55] E. G. C. P. van Loon, M. I. Katsnelson, and H. Hafermann, Phys. Rev. B **98**, 155117 (2018).
- [56] W. Metzner and D. Vollhardt, Phys. Rev. Lett. **62**, 324 (1989).
- [57] Q. Si and J. L. Smith, Phys. Rev. Lett. **77**, 3391 (1996).
- [58] See Supplemental Material at [URL will be inserted by publisher] for the case including nonlocal interactions and a discussion of the nonanalyticity of the Green's function.
- [59] S. Backes, J.-H. Sim, and S. Biermann, in preparation.
- [60] M. Potthoff, Eur. Phys. J. B **32**, 429 (2003).
- [61] J. Gukelberger, E. Kozik, and H. Hafermann, Phys. Rev. B **96**, 035152 (2017).
- [62] E. G. C. P. van Loon, F. Krien, H. Hafermann, E. A. Stepanov, A. I. Lichtenstein, and M. I. Katsnelson, Phys. Rev. B **93**, 155162 (2016).
- [63] G. Rohringer and A. Toschi, Phys. Rev. B **94**, 125144 (2016).
- [64] F. Krien, E. G. C. P. van Loon, H. Hafermann, J. Otsuki, M. I. Katsnelson, and A. I. Lichtenstein, Phys. Rev. B **96**, 075155 (2017).
- [65] M. Jarrell and J. Gubernatis, Physics Reports **269**, 133 (1996).

Non-local Correlation Effects in Fermionic Many-Body Systems: Overcoming the Non-causality Problem - Supplemental Material

Steffen Backes^{1,2,3,*}, Jae-Hoon Sim¹, and Silke Biermann^{1,2,3,4}

¹CPHT, CNRS, Ecole Polytechnique, Institut Polytechnique de Paris, Route de Saclay, 91128 Palaiseau, France

²Collège de France, 11 place Marcelin Berthelot, 75005 Paris, France

³European Theoretical Spectroscopy Facility, 91128 Palaiseau, France, Europe and

⁴Department of Physics, Division of Mathematical Physics,

Lund University, Professorsgatan 1, 22363 Lund, Sweden

(Dated: February 18, 2022)

THE GENERALIZED CAVITY EQUATIONS FOR NONLOCAL INTERACTIONS

The generalized DMFT equations derived in the main article considered nonlocal correlations in form of a nonlocal self-energy $\Sigma(k, i\omega)$. We can extend the derivation to nonlocal screenings in terms of a nonlocal polarization $P(q, i\nu)$ in the presence of nonlocal interactions. The general lattice action for a Hubbard model with nonlocal interactions is given by

$$S = \int_0^\beta d\tau \sum_{i\sigma} c_{i\sigma}^*(\tau) \left[\frac{\partial}{\partial \tau} - \mu \right] c_{i\sigma}(\tau) - \sum_{ij,\sigma} \int_0^\beta d\tau t_{ij} c_{i\sigma}^*(\tau) c_{j\sigma}(\tau) + \sum_i \int_0^\beta d\tau \tilde{n}_{i\uparrow}(\tau) v_{ii} \tilde{n}_{i\downarrow}(\tau) + \sum_{i<j} \int_0^\beta d\tau \tilde{n}_i(\tau) v_{ij} \tilde{n}_j(\tau), \quad (1)$$

where $c_{i\sigma}(\tau), c_{i\sigma}^*(\tau)$ are anticommuting Grassman variables, $\tilde{n}_{i\sigma}(\tau) = n_{i\sigma}(\tau) - \langle n_{i\sigma} \rangle$, $n_{i\sigma}(\tau) = c_{i\sigma}^*(\tau) c_{i\sigma}(\tau)$ and $\tilde{n}_i(\tau) = \sum_\sigma \tilde{n}_{i\sigma}(\tau)$. The hoppings t_{ij} and interactions v_{ij} are assumed to translationally invariant, e.g. $v_{ii} = v_{jj} \forall i, j$.

As discussed in the main text we split the action $S = S_0 + \Delta S + S^{(0)}$, where S_0 is the term that contains only the local quantities on site $i = 0$

$$S_0 = \int_0^\beta d\tau \sum_\sigma c_{0\sigma}^*(\tau) \left[\frac{\partial}{\partial \tau} - \mu \right] c_{0\sigma}(\tau) + \sum_\sigma \int_0^\beta d\tau t_{0\sigma} c_{0\sigma}^*(\tau) c_{0\sigma}(\tau) + \int_0^\beta d\tau \tilde{n}_{0\uparrow}(\tau) v_{00} \tilde{n}_{0\downarrow}(\tau). \quad (2)$$

The term ΔS contains all contributions that couples the site $i = 0$ to all other sites

$$\Delta S = - \sum_{j \neq 0, \sigma} \int_0^\beta d\tau (t_{0j} c_{0\sigma}^*(\tau) c_{j\sigma}(\tau) + t_{j0} c_{j\sigma}^*(\tau) c_{0\sigma}(\tau)) + \sum_{j \neq 0} \int_0^\beta d\tau \tilde{n}_0(\tau) v_{0j} \tilde{n}_j(\tau). \quad (3)$$

And finally, $S^{(0)}$ contains all the contributions of the lattice with site $i = 0$ and its bonds connecting it being removed

$$S^{(0)} = \int_0^\beta d\tau \sum_{i \neq 0, \sigma} c_{i\sigma}^*(\tau) \left[\frac{\partial}{\partial \tau} - \mu \right] c_{i\sigma}(\tau) - \sum_{ij \neq 0, \sigma} \int_0^\beta d\tau t_{ij} c_{i\sigma}^*(\tau) c_{j\sigma}(\tau) + \sum_{i \neq 0} \int_0^\beta d\tau \tilde{n}_{i\uparrow}(\tau) v_{ii} \tilde{n}_{i\downarrow}(\tau) + \sum_{\substack{i < j \\ ij \neq 0}} \int_0^\beta d\tau \tilde{n}_i(\tau) v_{ij} \tilde{n}_j(\tau). \quad (4)$$

Now integrating out all the degrees of freedom except the ones on site $i = 0$ one obtains an effective action of the form

$$S_{eff} = S_0 - \sum_{n=1}^{\infty} \frac{(-1)^n}{n!} \langle (\Delta S)^n \rangle^{(0)}, \quad (5)$$

where $\langle \rangle^{(0)} = \frac{1}{\mathcal{Z}^{(0)}} \int \prod_i dc_{i\sigma}^* dc_{i\sigma} e^{-S^{(0)}}$ indicates a trace over the system with the site $i = 0$ removed with a corresponding partition function $\mathcal{Z}^{(0)}$. In Ref.[1] it has been shown that with a rescaling of $t_{ij} \rightarrow t_{ij}/\sqrt{2d}$ and $v_{ij} \rightarrow v_{ij}v_{00}/\sqrt{2d}$, where d is the dimension of the lattice, that in the effective action all terms $n > 2$ vanish in the limit of $d \rightarrow \infty$.

The first order terms vanishes because the hopping term contains only expectation values of one Grassman variable, and the first order interaction term is proportional to $\langle \tilde{n}_{i\sigma} \rangle^{(0)} = \langle n_{i\sigma} \rangle^{(0)} - \langle n_{i\sigma} \rangle$, which is of order $1/d$. Additionally, different orders n have vanishing interference terms between the fermionic t_{ij} and density v_{ij} terms, thus there will be two separate series of terms for the t_{ij} and v_{ij} contributions. Thus, taking into account only the zeroth and the second order contribution we obtain an approximate form of the effective action which becomes exact in the $d \rightarrow \infty$ limit and evaluates to

$$\begin{aligned} S_{eff} &= S_0 - \frac{1}{2} \langle (\Delta S)^2 \rangle^{(0)} \\ &= \int_0^\beta d\tau_1 \int_0^\beta d\tau_2 \sum_\sigma c_{0\sigma}^*(\tau_1) \left(\delta(\tau_1 - \tau_2) \left[\frac{\partial}{\partial \tau} - \mu + t_{00} \right] + \sum_{ij \neq 0} t_{0i} t_{j0} G_{ij\sigma}^{(0)}(\tau_1 - \tau_2) \right) c_{0\sigma}(\tau) \\ &\quad + \int_0^\beta d\tau_1 \int_0^\beta d\tau_2 \tilde{n}_0(\tau_1) \left(\delta(\tau_1 - \tau_2) v_{00} - \sum_{ij \neq 0} v_{0i} v_{j0} \chi_{ij}^{(0)}(\tau_1 - \tau_2) \right) \tilde{n}_0(\tau_2). \end{aligned} \quad (6)$$

where we have introduced the cavity quantities

$$G_{ij\sigma}^{(0)}(\tau_1 - \tau_2) = - \langle T_\tau c_{i\sigma}(\tau_1) c_{j\sigma}^*(\tau_2) \rangle^{(0)} \quad (7)$$

$$\chi_{ij}^{(0)}(\tau_1 - \tau_2) = \langle \tilde{n}_i(\tau_1) \tilde{n}_j(\tau_2) \rangle^{(0)}. \quad (8)$$

This expression then takes the form of an impurity action

$$S_{eff} = - \int_0^\beta d\tau_1 \int_0^\beta d\tau_2 \sum_\sigma c_{0\sigma}^*(\tau_1) \mathcal{G}_\sigma^{-1}(\tau_1 - \tau_2) c_{0\sigma}(\tau) + \int_0^\beta d\tau_1 \int_0^\beta d\tau_2 \tilde{n}_0(\tau_1) U(\tau_1 - \tau_2) \tilde{n}_0(\tau_2), \quad (9)$$

with the effective Weiss field and interaction given by

$$\mathcal{G}_\sigma^{-1}(\tau_1 - \tau_2) = -\delta(\tau_1 - \tau_2) \left[\frac{\partial}{\partial \tau} - \mu + t_{00} \right] - \sum_{ij \neq 0} t_{0i} t_{j0} G_{ij\sigma}^{(0)}(\tau_1 - \tau_2) \quad (10)$$

$$U(\tau_1 - \tau_2) = \delta(\tau_1 - \tau_2) v_{00} - \sum_{ij \neq 0} v_{0i} v_{j0} \chi_{ij}^{(0)}(\tau_1 - \tau_2). \quad (11)$$

Or in the frequency domain

$$\mathcal{G}_\sigma^{-1}(i\omega) = i\omega + \mu - t_{00} - \sum_{ij \neq 0} t_{0i} t_{j0} G_{ij\sigma}^{(0)}(i\omega) \quad (12)$$

$$U(i\nu) = v_{00} - \sum_{ij \neq 0} v_{0i} v_{j0} \chi_{ij}^{(0)}(i\nu). \quad (13)$$

The connection to the original lattice including site $i = 0$ can be made by using the equations

$$G_{ij}^{(0)} = G_{ij} - G_{i0} G_{00}^{-1} G_{0j} \quad (14)$$

$$\chi_{ij}^{(0)} = \chi_{ij} - \chi_{i0} \chi_{00}^{-1} \chi_{0j}, \quad (15)$$

suppressing the spin index for readability. As discussed in the main text, one then arrives at the following expression for the Weiss field

$$\begin{aligned} \mathcal{G}^{-1}(i\omega) &= i\omega + \mu - \langle \epsilon \rangle - \left(\langle \epsilon G \epsilon \rangle - \langle \epsilon G \rangle \langle G \rangle^{-1} \langle G \epsilon \rangle \right) \\ &= \langle G \rangle^{-1} + \langle \Sigma \rangle - \left(\langle \Sigma G \Sigma \rangle - \langle \Sigma G \rangle \langle G \rangle^{-1} \langle G \Sigma \rangle + 2 \langle \Sigma \rangle - \langle \Sigma G \rangle \langle G \rangle^{-1} - \langle G \rangle^{-1} \langle G \Sigma \rangle \right). \end{aligned} \quad (16)$$

with $\langle \rangle$ indicating a local projection.

When comparing the effective interaction in Eq.(13) to the fermionic bath, we see that the bare interaction v formally plays the same role as the noninteracting hopping amplitude t , and the susceptibility χ takes the role of the

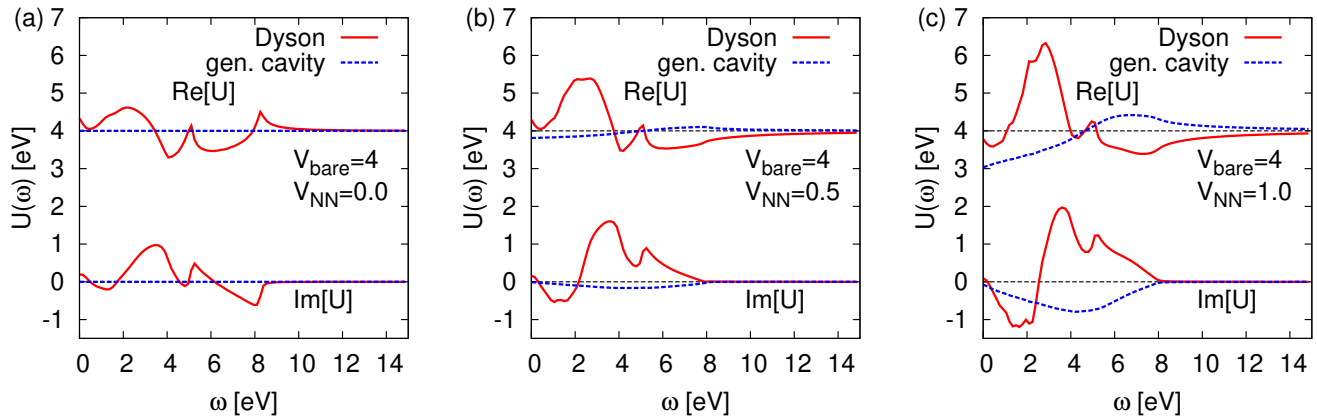


FIG. 1. The effective impurity interaction $U(\omega)$ on real frequencies ω for a two-dimensional single-orbital Hubbard model at half-filling for hopping $t = 1$, bare on-site interaction $V_{bare} = 4t$ for different values of the nearest-neighbor interaction V_{NN} . The polarization was obtained within the RPA approximation $P = G_0 G_0$. The interaction generated by the Dyson-like equation Eq.(23) shows noncausal behavior, indicated by $\text{Im}[U] > 0$, and unphysical screening effects for $V_{NN} = 0$. The generalized cavity equation Eq.(22) generates a causal interaction and obtains the correct limit of the bare interaction for the case of $V_{NN} = 0$.

single-particle Green's function G . Therefore, following the same derivation as for the single-particle Green's function the analogous result for the effective interaction is

$$U(i\nu) = \langle v \rangle - \left(\langle v\chi v \rangle - \langle v\chi \rangle \langle \chi \rangle^{-1} \langle \chi v \rangle \right). \quad (17)$$

This equation can be rewritten in terms of the screened interaction W and polarization P , by making use of the following identities

$$\chi = -P - PWP \quad (18)$$

$$v\chi = -PW \quad (19)$$

$$\chi v = -WP \quad (20)$$

$$v\chi v = v - W, \quad (21)$$

which leads to the following expression

$$U(i\nu) = [\langle W \rangle^{-1} + \langle P \rangle]^{-1} - \left(\langle PW \rangle [\langle P \rangle + \langle PWP \rangle]^{-1} \langle WP \rangle - \langle P \rangle \langle W \rangle [\langle P \rangle + \langle P \rangle \langle W \rangle \langle P \rangle]^{-1} \langle W \rangle \langle P \rangle \right). \quad (22)$$

We see that we obtain the usual local Dyson-like equation in the first term, but with an additional correction term. The correction term vanishes in case of a purely local polarization $P(q, i\nu) = P(i\nu)$, since the local projection separates $\langle PW \rangle = \langle P \rangle \langle W \rangle$ and the correction terms cancel each other, and we obtain the local Dyson-like equation

$$U(i\nu) = [\langle W \rangle^{-1} + \langle P \rangle]^{-1}. \quad (23)$$

Similar to the effective impurity bath Green's function \mathcal{G} , the effective impurity interaction U when generated from the Dyson-like equation Eq.(23) will show in general noncausal features in the presence of nonlocal polarization. Again, the additional term in Eq.(22) ensures causality as $\chi_{ij}^{(0)}$ is causal and thus implies causality of U if no further approximations are introduced. As an example we show the resulting effective interaction $U(\omega)$ for a two-dimensional single-orbital Hubbard model at half filling with hopping $t = 1$ and on-site bare interaction $V_{bare} = 4t$ for different values of a nearest-neighbor interaction V_{NN} in Fig.1. The polarization to screen the bare interaction has been generated using the RPA approximation $P = G_0 G_0$. Comparing the results of Eq.(22) and Eq.(23) we observe significant noncausal features in the effective interaction when the Dyson equation is used, indicated by positive values of the imaginary part of U . Here, the noncausal weight is in fact larger than the causal one. Additionally we observe an unphysical screening effect for a purely on-site interaction (Fig.1(a)) from the Dyson-like equation, which might explain similar reports in self-consistent dual boson calculations[2]. On the other hand, Eq.(22) generates a causal effective interaction, recovering the bare interaction for $V_{NN} = 0$, and enhanced screening for increasing nearest-neighbor interaction.

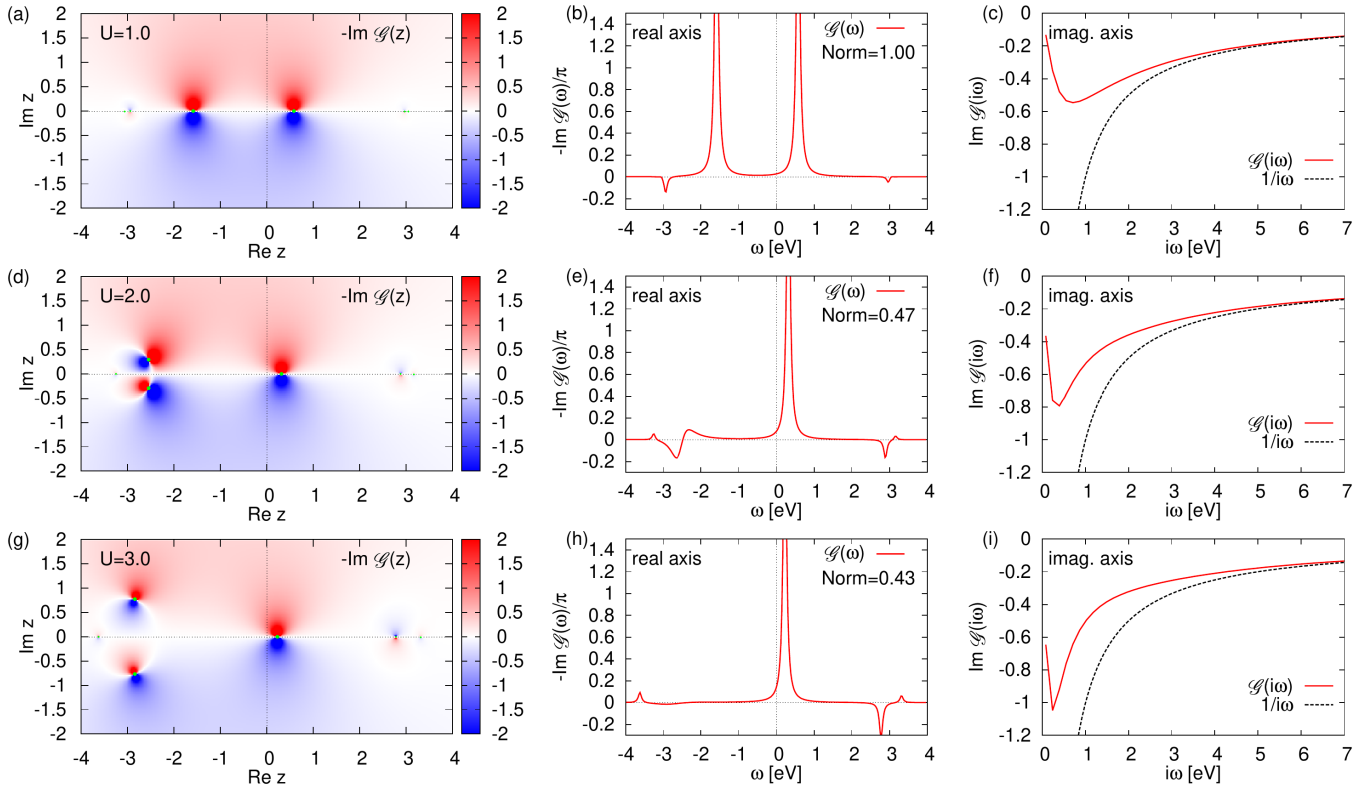


FIG. 2. The effective single-site impurity bath Green's function \mathcal{G} for the two-site dimer, generated from the exact solution using the impurity Dyson equation for the interaction (a)-(c) $U = 1t$, (d)-(f) $U = 2t$ and (g)-(i) $U = 3t$. The spectrum shown on the real axis corresponds to the limit in the upper complex plane $\omega + i0^+$. The poles of the Green's function in the complex plane are located between the red/blue extremal values, marked with a green dot. For small interactions the bath shows negative spectral weight but is normalized to one electron, since all poles of the Green's function are located on the real axis. For larger interaction values the poles of the Green's function move away from the real axis into the complex plane, reducing the normalization. Though, the Matsubara Green's function still shows a $1/i\omega$ behavior, indicating a violation of the Hilbert transform.

NONANALYTICITY OF THE IMPURITY MODEL

The problem of the emergence of a nonanalytic impurity solution in the upper/lower complex plane when the bath is generated from the Dyson equation is not related to the type of approximations involved, but occurs in general even for the exact solution. In order to see this and the resulting nonanalyticity (i.e., poles entering the complex plane), we show the single-site impurity bath Green's function \mathcal{G} for a dimer as discussed in the main text in the whole complex plane, generated from the exact self-energy in Fig.2. For all interaction values considered noncausal spectral weight, represented by negative values on the real axis, is present. For small interactions all poles of the Green's function are located on the real axis, but some of them have negative weight, as can be seen in Fig.2 (a) and (b) at $\omega = \pm 3$ eV. This negative spectral weight corresponds to negative hybridization amplitudes $|V|^2$, i.e. a purely imaginary and non-hermitian matrix element coupling the impurity to the bath.

As the interaction increases, two poles on the real axis merge and move into the complex plane, corresponding to two complex Eigenvalues $E_{\pm} = E_r \pm iE_i$. As a result the spectrum is not only noncausal as before, but also no longer normalized on the real axis. At the same time no features indicating such a behavior are visible in the Matsubara Green's function on the imaginary axis, which always shows a $1/i\omega$ decay for all interaction values. This represents a breakdown of the Hilbert transform

$$G(i\omega_n) = \int \frac{A(\omega)}{i\omega_n - \omega} d\omega, \quad (24)$$

which links the real frequency spectrum $A(\omega)$ to the Matsubara Green's function $G(i\omega_n)$. For large frequencies one obtains the relation between the normalization of the spectrum and the high-frequency behavior on the Matsubara

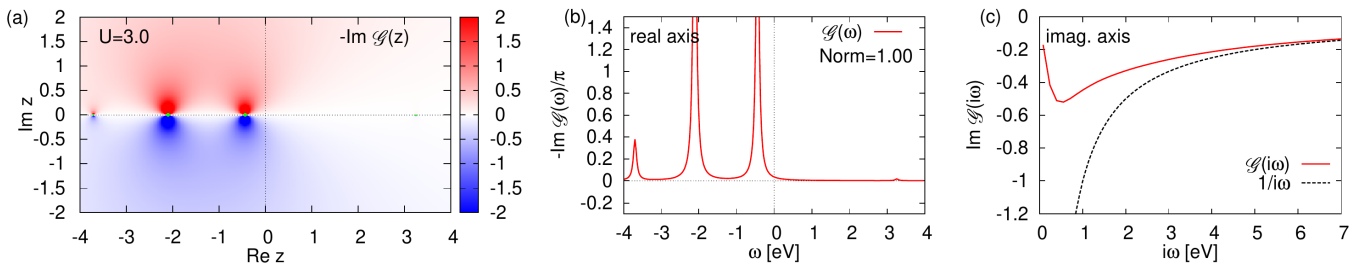


FIG. 3. The effective single-site impurity bath Green's function \mathcal{G} for the two-site dimer as in Fig.2, but generated from the generalized cavity DMFT equation Eq.(5) in the main text for $U = 3t$. No noncausal spectral weight is present and all poles of the Green's function are located on the real axis.

axis

$$G(i\omega_n) \approx \frac{1}{i\omega_n} \int A(\omega) d\omega, \quad \text{for large } \omega_n, \quad (25)$$

which is clearly violated for larger interactions in Fig.2 (f) and (i), as the tail of $\mathcal{G}(i\omega)$ indicates a normalization on the real axis equal to one. Such behavior is expected as the Hilbert transform only holds as long as the Green's function is analytic in the upper/lower complex plane, which is not the case when poles separate from the real axis into the complex plane. This is problematic as the real-frequency spectrum cannot be reconstructed by analytic continuation from the Matsubara Green's function by methods commonly used like the maximum entropy method [3], which relies on the Hilbert transform. Though, the Padé approximation[4] does not face this restriction and can still be applied, but is limited in practice due to a high sensitivity on numerical noise. We usually observed that the impurity solution, i.e. the impurity Green's function and self-energy exhibited even stronger nonanalytic behavior, with more poles leaving the real axis. As discussed in the main text, for $U = 3t$ all poles for the Selfenergy had left the real axis.

As described in the main text, the generalized cavity DMFT equations are causal. This is confirmed in Fig.3, which shows the effective bath Green's function for $U = 3t$. The spectrum is positive, normalized to one electron and the relation between the real and imaginary axis via the Hilbert transform still holds as the function is analytic in the whole upper complex/lower plane. This applies to all other derived quantities like the hybridization, impurity Green's function or self-energy.

* steffen.backes@polytechnique.edu

[1] Q. Si and J. L. Smith, Phys. Rev. Lett. **77**, 3391 (1996).

[2] E. A. Stepanov, E. G. C. P. van Loon, A. A. Katanin, A. I. Lichtenstein, M. I. Katsnelson, and A. N. Rubtsov, Phys. Rev. B **93**, 045107 (2016).

[3] M. Jarrell and J. Gubernatis, Physics Reports **269**, 133 (1996).

[4] H. Padé, Ann. Sci. École Norm. Sup. Suppl. (3) **9** (1892).